Precision DSN Radiometer Systems: Impact on Microwave Calibrations

CHARLES T. STELZRIED, SENIOR MEMBER, IEEE, AND MICHAEL J. KLEIN

The NASA Deep Space Network (DSN) has a long history of providing large parabolic dish antennas with precision surfaces, low-loss feeds, and ultra-low noise amplifiers for deep-space telecommunications. To realize the benefits of high sensitivity, it is important that receiving systems are accurately calibrated and monitored to maintain peak performance. A method is described to measure system performance and to calibrate the receiving system using procedures, software, and commercial instruments that are easy to implement and efficient to use.

The utility of the measurement procedures and the precision of the receiver calibration technique were demonstrated by performing tests at K_a-band (32 and 33.68 GHz) frequencies at Goldstone on a 34-m beam-waveguide antenna. Observations of multiple calibration radio sources are used to measure the dependence of antenna gain and system noise temperature on source elevation and derive the performance parameters.

Receiving system nonlinearities are frequently overlooked as an error source in the calibration of microwave radiometers. The experimental results described in this paper illustrate some of the ways that receiving system nonlinearity can negatively impact system performance. A simple radiometer calibration technique and analysis provide quantitative information that enables the system engineer to adjust and linearize the receiving system. When that is not practical, the experimenter or the operator can apply correction coefficients to the measured values of system noise temperature and thereby compensate for the receiving system nonlinearity.

The high-performance antennas and the sensitive receiving systems of the DSN are valuable resources for scientific research in addition to the primary telecommunication tasks that support space missions. The antenna gain and system noise temperature measurements and the radiometer calibration method described in this paper are also useful to perform precision research experiments.

I. INTRODUCTION

The NASA Deep Space Network (DSN) has a long history of providing sensitive receiving systems for deep-space communications. These systems include large parabolic dish antennas with precision surfaces, low-loss feeds, and ultra-low-noise amplifiers. The sensitivity of these systems is characterized by measuring the receiving system figure of merit parameter $G/T_{\rm op}$ [1], [2] where G is the antenna gain and $T_{\rm op}$ is the system operating noise temperature [3]. $T_{\rm op}$ includes contributions from cosmic noise, atmospheric emission, feed system losses, and the receiving system thermal noise. The larger the $G/T_{\rm op}$ value, the more sensitive the system for spacecraft communications, radio and radar science, and radio astronomy.

Over the past several decades the $G/T_{\rm op}$ parameter of microwave receiving systems has dramatically increased in the wake of technological developments and improved engineering practices. The $G/T_{\rm op}$ for a microwave receiving system is optimized and calibrated and periodically monitored to detect potential degradation in performance. Potential sources of degradation include inclement local weather, physical antenna damage following severe rain and wind storms or, more rarely, earthquakes and routine modifications to the antenna feed and/or receiving subsystems.

Deep-space planetary missions need reliable and current information of $G/T_{\rm op}$ to specify spacecraft telemetry data rates. The DSN, with 26-, 34-, and 70-m antennas, schedules the appropriate antenna size and performance to match the mission requirements. During critical mission phases such as planetary flybys, it is especially important to match antenna performance to the mission telecommunications requirements.

In this paper a set of routine procedures is developed to monitor the $G/T_{\rm op}$ parameter using radio sources and radiometers with high precision and minimal calibration time. Examples of performance measurements of the new NASA DSN Goldstone DSS 13 R&D 34-m beam-waveguide (BWG) antenna are presented and discussed. The data are analyzed to study the effects of receiver nonlinearity on system performance. Considerable attention is given user-friendly methods to verify and correct for receiving system nonlinearity.

II. CALIBRATING LARGE MICROWAVE ANTENNAS

A. The $G/T_{\rm op}$ Parameter

The $G/T_{\rm op}$ ratio is an accepted and useful parameter to quantify the sensitivity of microwave receiving systems

Manuscript received May 3, 1993; revised November 15, 1993.The research reported in this paper was performed by the Jet Propulsion Laboratory, California Institute of Technology, Pasadena, under contract with the National Aeronautics and Space Administration.

The authors are with the Jet Propulsion Laboratory, California Institute of Technology, Pasadena, CA 91109.

IEEE Log Number 9400206.

that use large collecting areas and low-noise microwave amplifiers [1], [2], [4]. The gain of reflector microwave antennas is proportional to the collecting area of the surface divided by the square of the received wavelength [5]. The system noise temperature is the result of several contributing sources. The $G/T_{\rm op}$ parameter is defined by

$$G/T_{\rm op} = \frac{4\pi A_e \lambda^{-2}}{T_a + T_e} \tag{1}$$

where A_e is the effective antenna area, λ is the received wavelength, $T_{\rm op} = (T_a + T_e)$ is the system operating noise temperature [3], [4], T_a is the antenna noise temperature with contributions from the 2.73 K cosmic background, the earth's atmosphere ($T_{\rm atm}$) and the antenna transmission line (T_t), and T_e is the effective noise temperature of the receiving system with contributions from the low-noise amplifier ($T_{\rm lna}$), and the follow-up amplifier (T_f).

Precision measurements of the $G/T_{\rm op}$ of DSN antennas and their associated receiving subsystems are usually made when a new antenna is completed, when a significant upgrade is made to an existing antenna, and on a periodic basis for monitoring purposes. An effective method of obtaining $G/T_{\rm op}$ for microwave receiving systems is to measure the increase of the system noise when the antenna is pointed at a source of microwave emission with a known power density. In practice, the calibration source is usually selected from a list of astronomical radio sources whose microwave spectra have been accurately measured. The relationships between $G/T_{\rm op}$, the power ratio measurement, and the flux density of the calibration radio source are developed below.

The power ratio measurement is expressed as a Y-factor

$$Y = (T_{\rm op} + T_s)/T_{\rm op} \tag{2}$$

where T_s is the increase in system noise temperature when the antenna is pointed at the radio source given by

$$T_s = SA_e/2k \tag{3}$$

where S is the flux density of the radio source $(\mathrm{J \cdot m^{-2}})$[1], k is the Boltzmann constant (1.3807×10^{-23} $\mathrm{J \cdot K^{-1}}$), and

$$G = 4\pi A_e/\lambda^2. \tag{4}$$

Substituting these equations into (1)

$$G/T_{\rm op} = (Y - 1)(8\pi k/k_1 C_r \lambda^2 S) \tag{5}$$

where k_1 and C_r are constants accounting for transmission losses through the atmosphere and for the loss in received power for those cases where the angular dimensions of the radio source are partially resolved by the antenna beam, i.e., the angular dimensions of the calibration radio sources are small but they are not "point" sources. From (5) it is clear that $G/T_{\rm op}$ can be calculated from the Y-factor measurement when the flux density S of the radio source is known. In practice, $G/T_{\rm op}$ for systems with large steerable antennas changes significantly as the pointing angle varies from horizon to zenith. The atmospheric component of system noise temperature increases with increasing zenith angle (decreasing elevation angle) while gravity distorts the structure as the antenna is tilted away (up or down) from the rigging angle (usually 45°) where G is maximized by adjusting the surface panels. The dependence of $G/T_{\rm op}$ on elevation angle is usually measured from a series of observations of one or more radio sources over a wide range of elevation angles. The process usually requires more than 6 h and often several days to complete.

The typical DSN antenna is instrumented with several receiving subsystems operating at different frequencies. Scheduling the time to calibrate $G/T_{\rm op}$ for each DSN frequency band can be accommodated on an occasional basis, but routine monitoring is problematic. For the DSN, monitoring $G/T_{\rm op}$ is simplified by measuring G and $T_{\rm op}$ separately. G and its elevation dependence are assumed to be stable with time. $T_{\rm op}$ is routinely monitored in the DSN as part of the spacecraft telecommunications procedures.

B. Calibration Radio Sources

The current method of calibrating operational DSN antennas using astronomical radio sources was standardized and documented after upgrading the 64-m subnet to 70-m-diameter antennas [6]. The use of radio sources for this purpose has been in use for decades by the radio astronomy community and has been adopted by the DSN. This method measures the antenna gain by using the broadband flux densities of a selected set [7]–[10] of galactic and extragalactic radio sources sufficiently well-known to be used as calibration standards. The advantage of this approach is that these astronomical radio sources, which are distributed over the entire sky, can be measured day or night at virtually any position in the sky. The method has been used very successfully to measure the relative changes in antenna gain versus elevation angle as the radio sources rise and set.

A difficulty of this approach involves the accuracy of the measurements, which depends upon knowledge of the radio flux densities, the angular size of the emission region, and the intensity variations with time. Fortunately, enough is known about the list of calibration sources so that measurements of relative changes can be made with 2-sigma precision of approximately 0.15 dB and measurements of absolute gain can be made with a 2-sigma accuracy of approximately 0.5 dB.

Source lists for calibration at frequencies above 20 GHz often include the brighter planets such as Venus and Jupiter. In contrast with most astrophysical radio sources, the flux density of a planet increases rather than decreases with increasing frequency and for this reason planets tend to be the strongest continuum radio sources at wavelengths shorter than about 1 cm. Furthermore, the flux densities from planetary atmospheres and/or surfaces can be calculated from detailed thermophysical models developed from data returned by numerous spacecraft that have been sent from Earth.

[1] S is usually expressed in janskys where 1 Jy = 10^{-26} $\mathrm{J \cdot m^{-2}}$.

III. A Practical Method to Determine G/T

A. Receiving System Calibration Instrumentation

The operational Deep Space Network (DSN) uses noise adding radiometers (NAR's) to perform antenna gain and noise temperature calibrations for telecommunications performance analyses [6]. The NAR configuration, developed in the 1970's, uses a microwave noise diode as a reference to compensate for gain fluctuations in the maser low-noise amplifier (LNA). The sensitivity of the NAR configuration is significantly better than the total power radiometer (TPR) configurations that it replaced. It has been successfully used in the DSN for almost two decades.

As part of an effort to provide DSN operators with efficient and convenient methods to maintain accurate calibrations of microwave radiometers, a modest research and development activity was carried out at the Goldstone DSS 13 Venus R&D station. The objective was to develop user-friendly methods to measure system noise temperature and antenna gain with improved accuracy and to replace special-purpose detectors and computers with commercially available equipment.

The development work began with a NAR configuration similar to those used in the operational DSN. A TPR, which uses a commercial digital power meter detector, was also assembled and tested because it had the potential of being a more reliable and cost-effective configuration. TPR's are now competitive with gain-stabilized systems, such as the NAR, because of recent advances in low-noise amplifiers and follow-on receiver hardware as well as improvements in modern computer technology that accommodate frequent radiometer calibrations as part of the observation data strategy.

Figure 1 represents the TPR configuration that was used to develop and test calibration techniques at the Venus Station on the 26-m antenna at S- and X-band (2.3 and 8.4 GHz) and recently on the new 34-m beam-waveguide (BWG) antenna at X-band (8.4 GHz) and K_a-band (32 and 33.68 GHz); see [11]–[14]. The radiometer system includes the antenna feed, an ambient temperature load, a microwave switch, a linearity calibration noise diode, a readout device, and a receiving system. The readout device for the TPR is a Hewlett-Packard 438-A digital power meter. The receiving system usually consists of an LNA, mixer, and IF amplifiers. The signal level is adjusted to provide an output of about 2 μW when the microwave LNA input is connected to the ambient load.

The ambient load has traditionally been a waveguide termination that is accessed through the waveguide switch. This configuration was modified to take advantage of the benign environment of the instrumentation room located in the basement of the BWG antenna. The waveguide switch was removed and the waveguide load was replaced with an aperture load attached to a movable arm designed to swing the load in a plane located above and perpendicular to the feed aperture. The insertion loss of the microwave feed assembly is reduced with the removal of the waveguide switch.

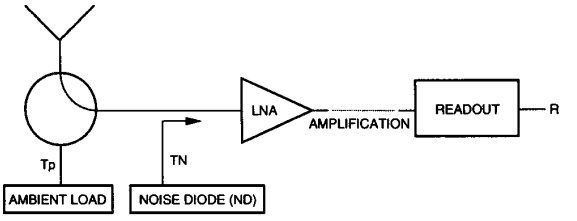

Fig. 1. Microwave total power radiometer (TPR) block diagram.

The gain of the TPR receiving system will usually drift with time and/or changes in ambient temperature. Experience has shown that modern LNA's, follow-on amplifiers, and commercial power meter detectors are stable for short-term variations (1 min). However, it is very important to account for long-term drifts in the end-to-end gain of the TPR receiving system. Extensive tests of a variety of TPR receiving systems used at Goldstone over the past five years have demonstrated that gain drifts are relatively small ($< 5\%$ over several hours) and sufficiently slow that gain variations can be accurately tracked if calibrations are made two or three times per hour. These "observing calibrations" or "minicals" require less than 1 min to complete, so they are only minor interruptions to the observational sequence. An example of a typical calibration sequence is discussed in Section IV-A.

The method applies equally well to an NAR with a square-law detector or to a Dicke switching system with a phase-sensitive detector. For the NAR system, a second noise diode is needed to provide the noise modulation at the LNA input.

B. The Radiometer Calibration Method

The radiometer calibration data are recorded from the readout device as the system is configured to five different states. The readout, $R1$, of the first state is the bias with the readout device input terminated in a matched load. Ideally $R1$ should be exactly zero, but in some configurations it has a small but nonzero value. The second and third states are recorded with the LNA input connected to the antenna and the antenna is directed at the cold sky with the noise diode off ($R2$) and diode on ($R3$). The LNA input is then connected to the ambient load for the fourth and fifth states where $R4$ is recorded with the diode off and $R5$ is recorded with the diode on. The readout device bias $R1$ is subtracted from each of the other four readouts before subsequent computations are made. Figure 2 is a schematic showing the relationship between system readout (with bias reading removed) and input-noise temperatures for a linear system and a hypothetical system with severe nonlinearity.

When the ambient termination is properly matched, the system noise temperature with the receiving system input connected to the ambient load is given by

$$T4 = T_p + T_e \tag{6}$$

where T_p is the physical temperature of the termination (load) which is typically measured with a digital ther-

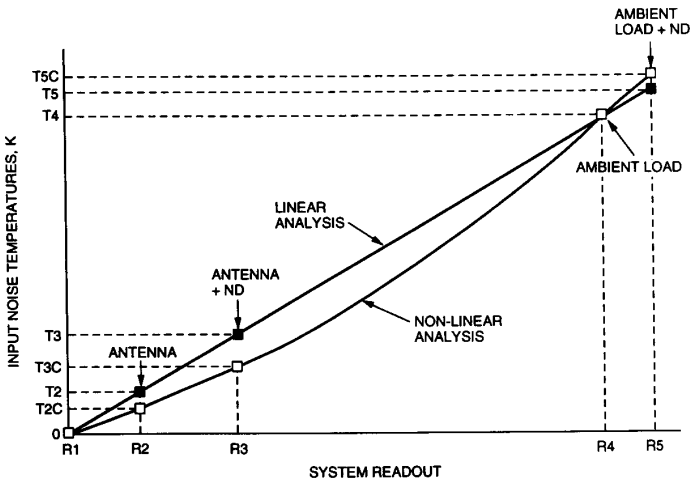

Fig. 2. Schematic input system noise temperatures and output readings for a total power radiometer. The results of a linear and nonlinear analysis example are shown.

mometer, and T_e is the receiving system noise temperature, which is assumed known from separate calibrations. In low-noise systems T_e is small compared to T_p so that a small percentage error in T_e contributes a smaller percentage error in $T4$ [15]. For example, if $T_p = 290$ K and $T_e = 10$ K, a 10% error in T_e results in only a 0.33% error in $T4$.

The radiometer receiving system gain is defined by the ratio

$$B = T4/R4. \tag{7}$$

Assuming the system is linear, the system noise temperature with the LNA input connected to the antenna is given by

$$T2 = B \cdot R2 \tag{8}$$

where $T2 = T_{\text{op}}$ with the antenna pointing at a "cold sky" calibration position, which in many cases is near the zenith. If a radiometer receiving system is not linear, the relation between T and R will deviate from the simple proportion of (8) as discussed in the Appendix. To compensate for the deviation, the corrected system noise temperature on the antenna is defined by

$$T2C = BC \cdot T2 + CC \cdot T2^2. \tag{9}$$

The constants BC and CC are calibrated using the noise diode associated with readings $R3$ and $R5$ described above. The linearity of the receiving system is evaluated by comparing the two readout increments ($R5$-$R4$) and ($R3$-$R2$). For a perfectly linear system, these two increments will be equal and the two constants will be $BC = 1$ and $CC = 0$. A quantitative indication of a nonlinear system is given by the magnitude of the difference between $T2C$ and $T2$. Details of the method and the analysis are given in the Appendix.

Tests made with nonlinear systems suggest that (9) can be used for post-observing radiometer nonlinearity error corrections whenever stable, calibrated values for the constants BC and CC are known

$$T_{\text{op}}(\text{corrected}) = T_{\text{op}}C = BC \cdot T_{\text{op}} + CC \cdot T_{\text{op}}^2. \tag{10}$$

However, the best practice is to identify the receiver nonlinear elements and then adjust the system operating conditions for linear performance (see Section III-C).

C. The Issue of Radiometer Dynamic Range

The radiometer receiving system nonlinear performance has proven to be a troublesome component of the error budget for the measurement of DSN antenna parameters. An example of the problem surfaced when it was discovered that system temperature measurements taken with the NAR did not agree with those taken with the TPR. The problem persisted even when the NAR algorithms were adjusted to compensate for nonlinearity in the square-law detector (use of an "alpha" coefficient, described in [16]). Further analysis indicated that radiometer receiving system nonlinearity might explain the conflicting results and the test procedure was modified to measure the end-to-end linearity of each radiometer receiving system configuration.

The utility of the test procedure was demonstrated at Goldstone in November 1992 when a K_a-band receiving system was installed on the 34-m BWG antenna at DSS 13. A TPR system was implemented with a 32-GHz maser low-noise amplifier in the BWG pedestal room and the calibration tests described in this paper were carried out. The data corresponding to the five measurement states are shown graphically in Fig. 3. The results, which gave system temperatures of $T2 = 50.6$ K and $T2C = 45.7$ K, indicated that the receiving system nonlinearity (obtained from $T2/T2C$) was approximately 11% as measured on 11/10/92. Attenuator pads were inserted at the inputs to key elements in the receiver amplifier chain to optimize the gain profile and linearity of the system. When the calibration

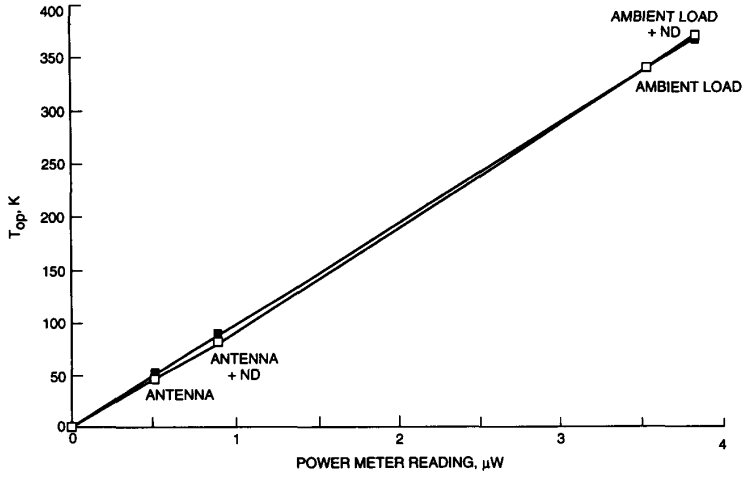

Fig. 3. Experimental results from a total power radiometer linear and nonlinear analysis as a function of uncalibrated radiometer output readings taken 11/10/92 on the DSS 13 34-m antenna K_a-band nonoptimized receiving system configuration.

procedure was repeated (11/18/92), the measured system temperatures of $T2 = 46.0$ K and $T2C = 45.6$ K indicated nonlinearity less than 1%. It is interesting to note that the values of $T2C$ before and after reducing the receiving system nonlinearity agreed within 0.1 K (also less than 1%) providing confidence in this calibration method. These results demonstrate that the optimization and calibration sequence is effective.

The nonlinearity of the receiving system shown in Fig. 3 might not appear to be severe at first glance. However, an 11% nonlinearity produces significant degradations to the error budget of system performance measurements. Moreover, these effects tend to be systematic rather than random, so they are often overlooked.

An example of the insidious impact of receiving system nonlinearity is illustrated in Fig. 4 where the values of $T2$ (linear analysis) and $T2C$ (nonlinear analysis) are plotted for three different radiometer test configurations on the 26-m antenna at DSS 13 in 1987. The objective was to compare the calibration results of an NAR and two TPR systems using the linear and the nonlinear analysis methods [17]. The NAR and one of the TPR systems used a detector that was known to be several percent nonlinear. The TPR with a power meter detector was expected to be the most linear and the most accurate of the three configurations.

The results of the three calibrations with linear analysis gave $T2$ values (solid dots) that fell in the range of 30.8 to 31.9 K. In contrast, the nonlinear analysis produced results that converged to $T2C = 31.85 \pm 0.05$ K (open circles). This average value of $T2C$ was very close to the value of $T2$ for the TPR configuration that was believed to be the most linear at the outset.

Receiving system linearity is important to verify and easy to overlook when new systems are installed or when existing systems are modified. The calibration method described in this section is an efficient technique to evaluate and monitor end-to-end receiving system linearity.

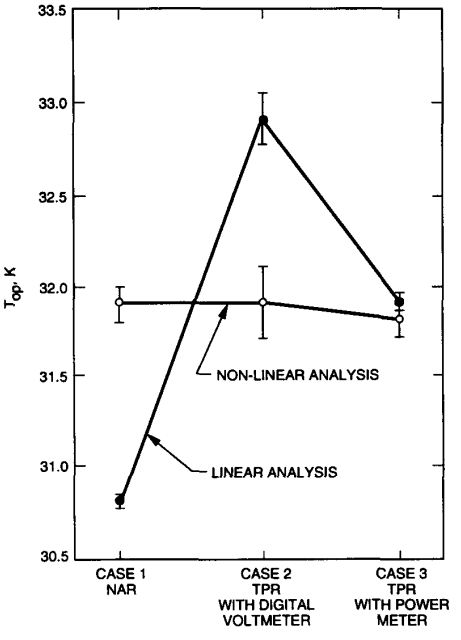

Fig. 4. Comparison of results from a linear and nonlinear analysis applied to the zenith noise temperature calibrations using the NAR and TPR on the DSS 13 26-m antenna at 2.3 GHz (8/28/87).

IV. Testing, Verifying, and Application

A. Test Observations

The DSS 13 Venus station provides a facility to test instrumentation and verify the analysis used to measure system noise temperature and antenna efficiency. In March 1993, a K_a-band HEMT low-noise amplifier was installed at one of the receiving system stations in the pedestal room of the BWG 34-m antenna. The TPR system described in Section III-A was implemented to test the system at

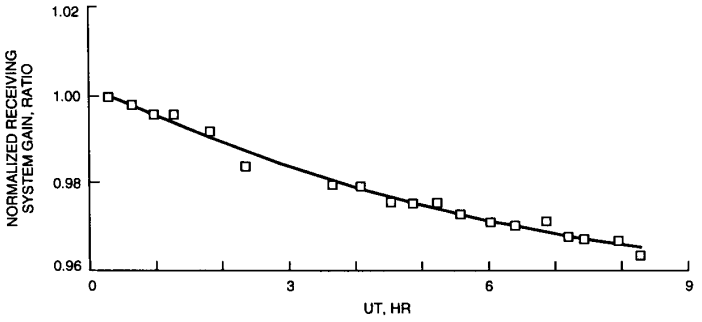

Fig. 5. Calibration of the time dependence of receiving system gain of the HEMT LNA/receiver operating at 33.68 GHz on the DSS 13 34-m BWG antenna. Calibrations were made with the OBSCAL program on 4/1/93 (DOY 091).

33.68 GHz. The detector is a Hewlett-Packard 438-A digital power meter which is specified to provide linearity better than 99%. Evaluating the receiving system linearity was one of the test objectives of the calibration measurements.

The radio sources selected for the calibration tests were Venus, Jupiter, and the radio Galaxy Virgo A, which is one of the better understood radio sources used for antenna gain measurements. Venus and Jupiter are "bright" K_a-band radio sources, where flux densities can be calculated with estimated 2–sigma accuracy of ±8% (absolute flux scale). Furthermore, these particular sources were selected because their flux densities differed by a wide margin from the weakest (Virgo A at 14 Jy) to the strongest (Venus at 1060 Jy). This range of source intensities proved to be useful for the receiving system linearity tests described in Section IV-C.

The 1993 observations were made between 0 and 08 hours UT on April 1 (DOY 091) and between 22 hours UT April 7 and 09 hours UT on April 8 (DOY 098). The radio source noise temperatures were measured using a two–coordinate 5-point antenna pointing sequence. The TPR measures and records T_{op} while the antenna beam pointing offset is zero in one coordinate and the beam position is stepped through 5 offset positions $(x_1 \cdots x_5)$ in the orthogonal coordinate. The offset values are $x_i = n_i \times$ HPBW, where $n_i = +5, +0.5, 0, -0.5, -5$ and HPBW = one half-power beam-width (the full width between ± 3-dB points). The ten values of T_{op} are then processed to evaluate the peak source temperature and adjust for residual pointing offset errors, which were typically less than ± 0.1 HPBW.

Precision calibration sequences of the radiometer were conducted before (PRECAL) and after (POSTCAL) the observing sessions on the two dates. The data for each PRECAL and POSTCAL consists of a set of six measurements of $R1$ through $R5$ described in Section III-B. The results are average values and standard deviations of the TPR receiver gain and system linearity coefficients (B, BC, and CC).

The TPR receiving system gain calibration was remeasured periodically at least twice each hour through the observing session. The results of these "observing calibrations" (OBSCAL) were used to update the TPR receiving system gain coefficients and thereby compensate for slow variations of gain. The April 1 OBSCAL receiving system gain data, expressed as ratios relative to the PRECAL gain, are shown in Fig. 5. The trend and the scatter of the data are representative of calibration data taken on many occasions. Experience has shown that errors in the updated TPR receiving system gain are usually less than 0.5% when this procedure is followed.

The PRECAL and POSTCAL data were combined to evaluate the TPR system linearity for the two dates. The results show that the receiving system nonlinearity was < 1% during these observations: $T2/T2C = 0.992$ on April 1 and 0.994 on April 7/8. The PRECAL results were within ± 0.001 of the POSTCAL results on both days.

B. Aperture Efficiency Results

The radio sources were observed over a wide range of elevation angles to calibrate the changes of aperture efficiency as the antenna pointing angles vary from horizon to zenith. The aperture efficiency η is the ratio of the effective aperture A_e and the geometric aperture A_g of the parabaloid.

$$\eta = A_e/A_g = 4A_e/\pi D^2 \tag{11}$$

where D is the aperture diameter. Substituting (3) (Section II-A), (11) can be rewritten

$$\eta = 8kT_s^*/\pi D^2 S \tag{12}$$

where

$$T_s^* = C_r T_s \tag{13}$$

and $C_r \geq 1$ is a correction factor applied to the observed source antenna temperature, T_s, to adjust for the loss in signal that occurs when the antenna beam partially resolves the solid angle of the source, which is either a circular or elliptical disc when the source is a planet.

Individual values of η for each measurement of T_s can be calculated for known values of flux density (S) and C_r that are listed in Table 1. The value of $C_r = 1.28 \pm 0.02$ for Virgo A was measured in August 1993 by comparing two-dimensional brightness temperature maps of Virgo A and the quasar radio source 3C 273, which is sufficiently

Table 1 Source Flux Densities and Peak Temperatures

Common Name	IAU Designation	S(33.68GHz) (Jy)	Reference	C_r	T(Source) (eff=100%)
Venus (Apr. 1)	–	1051.8	[18]	1.342	257.6
Venus (Apr. 8)	–	1004.1	[18]	1.326	249.1
Jupiter (Apr. 1)	–	164.3	[19], [20]	1.168	46.25
Jupiter (Apr. 8)	–	163.6	[19], [20]	1.167	46.10
Virgo A (3C 274)	1228 + 126	14.1	[6]	1.28	3.608

Note 1: Planet fluxes were calculated from referenced disc brightness temperatures [Venus T_b = 460 K; Jupiter T_b = 140 K] with compensation for the planet's distance from Earth.
Note 2: IAU = International Astronomical Union

compact to serve as a "point source" calibrator for the 34-m antenna at K_a-band frequencies.

Combining (11) and (12), and setting $\eta = 1$ gives an expression for source temperature for a "perfect" antenna

$$T_s(100\%) = \pi D^2 S/8kC_r = 2.8442 \times 10^{22} D^2 S/C_r. \tag{14}$$

A useful alternative expression for the aperture efficiency is

$$\eta = T_s/T_s(100\%). \tag{15}$$

Values of $T_s(100\%)$ are shown in the last column of Table 1.

The aperture efficiency measurement data are plotted as a function of elevation angle in Fig. 6. Each value of T_s was adjusted to compensate for the attenuation by the terrestrial atmosphere. The attenuation is compensated from ground weather parameters assuming a horizontally stratified flat-earth model for the troposphere and a simple (1/sin) dependence on elevation angle [21]. The efficiency peak of 0.43 near elevation angle 55° matches the curves from the more extensive measurements reported in [22] and summarized in [1].

The data associated with the three calibration sources, identified by different symbols in Fig. 6, are consistent. The agreement can be quantified by separating the data into three sets and independently solving for the peak aperture efficiency. The results from the calibration observations taken at 33.68 GHz are listed in column 3 of Table 2. The corresponding values of the peak antenna gain are listed in the fourth column. The average value of the peak gain is 77.94 dB and the corresponding $G/T_{\rm op}$ is 59.08 dB, where $T_{\rm op}$ = 77 K is the average system temperature that was observed near 55° elevation.

The peak efficiencies for the three sources differ from the average value by less than 0.005. This result suggests that the microwave spectra of the two planets at short centimeter wavelengths have been accurately calibrated and that the measured value of C_r for Virgo A leads to a consistent result for that source as well. Absolute calibration measurements of the K_a-band spectra of these three sources are the subjects of a current study by the authors of [23].

For the present DSS 13 34-m antenna HEMT LNA configuration, $T_{\rm op}$ = 77 K at 55° elevation angle. This

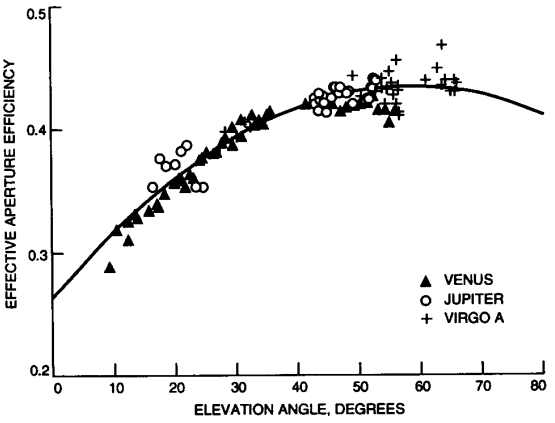

Fig. 6. The measured dependence of the effective aperture efficiency η on radio source elevation for the DSS 13 34-m antenna operating at K_a-band (33.68 GHz); attenuation from the clear atmosphere has been removed.

Table 2 Calibration Results at 33.68 GHz for 34-m Beam Waveguide Antenna at DSS 13 (Goldstone)

Source Name	Peak T_s (K)	Peak Efficiency	Peak Gain (dB)
Venus	110	0.431	77.92
Jupiter	19.9	0.432	77.93
Virgo A	1.57	0.436	77.97
Averages:		0.433	77.94

results in a peak estimate of $G/T_{\rm op}$ = 59.08 dB for K_a-band near 55° elevation angle, but $G/T_{\rm op}$ actually peaks at a slightly higher elevation angle because the system noise temperature varies from a maximum at low antenna elevation angles to a minimum at zenith.

C. Receiving System Nonlinearity Effects

The agreement of the data in Fig. 6 and Table 2 would not have been so close had a nonlinear receiving system

Table 3 Example of Errors Caused by 11 % Nonlinearity in an Unoptimized TPR System—DSS 13 34-m Antenna Radio Source T_s Calibration Nonlinearity Measurement Errors with Unoptimized Radiometer System Based on 11/10/92 Evaluation

Hypothetical Source Temperatures, T_s			
T_s, K	T_{off} = 30 K	T_{off} = 50 K	T_{off} = 70 K
	T_s Measurement Errors, %		
10.	9.9	8.3	6.8
100.	6.4	4.9	3.5
200.	2.7	1.4	0.0

Table 4 Example of Errors Caused by 11 % Nonlinearity in an Unoptimized TPR System—Effect that 11% Radiometer Nonlinearity Would Have Had on Antenna Gain Calibration Measurements of April 1993

Sources Observed in April 1993			
Sources	T_{off} = 30 K	T_{off} = 50 K	T_{off} = 70 K
	Hypothetical Antenna Gain Measurement Errors, dB		
Virgo A	0.45	0.38	0.31
Jupiter	0.41	0.34	0.28
Venus	0.27	0.21	0.14

been used for the observations because the errors introduced by radiometer nonlinear performance are not uniform with source temperature magnitude.To demonstrate this dependence, the data taken in November 1992 with the nonlinear receiving system described in Section III-C were subjected to the linear and the nonlinear analyses.

The percentage error caused by the nonlinearity, given by (A16) in the Appendix, is a function of the calibration temperatures $T4$, T_{off}, (system noise temperature with antenna off pointed in the region of a nearby radio source calibrator), T_s (the radio source noise temperature contribution), and the linearity coefficient CC. For the 11/10/92 data, $T4 = 340.1$ K and $CC = 3.33394 \times 10^{-4}$ and $T_{off} = 50.6$ K. Using these parameters, the percentage error in measurements of T_s were calculated for hypothetical values of T_s in the range 10 to 200 K. The results are shown in the Appendix (Fig. 8) and summarized here in Tables 3 and 4 for three values of the system temperatures near zenith that are representative of a HEMT ($T_{off} = 70$ K), the maser/dichroic configuration of November 1992 ($T_{off} = 50$ K), and the maser/dichroic configuration ($T_{off} = 30$ K) that is expected to be realized in the future at DSS 13 [24].

An example of the impact of radiometer receiving system nonlinearity on antenna gain measurements is shown in Table 4. Had the gain measurements of April 1993 been made with a 11% radiometer nonlinearity, the results for the three sources would have been in error by the amounts listed in the last column of Table 4 ($T_{off} = 70$ K). The hypothetical TPR nonlinearity would have caused the antenna gain results from the three sources to diverge as the nonlinearity-caused antenna measurement error increased from 0.14 dB for Venus to 0.31 dB for Virgo A. The average value of the gain would have been incorrect and the scatter of the three data values would have been 2.8 times greater than the variance of the experimental data.

TPR receiving system nonlinearity errors are increased as the system noise temperature decreases and are minimized for source temperatures $T_s = T4 - 2T_{off}$.

D. Receiving System Nonlinearity Effects and Variable Radio Sources

Measurements of radio source flux densities with nonlinear TPR receiving systems may produce pathological results that are exacerbated if the radio source intensity is time-variable. Many galactic and extragalactic radio sources are known to exhibit intensity variations, and measurements of these sources will be biased by the nonlinear errors that arise as T_s changes. The effect is small (<0.1 dB) for most sources because the amplitude of the intensity variations is usually much less than 50%

Receiving system nonlinearities produce errors that may be surprisingly large when the brighter planets are observed at short centimeter or millimeter wavelengths. A prime example of the problem can be derived from the 1993 Venus measurement at 33.68 GHz. The observations were made when Venus was near inferior conjunction, i.e., the time when the distance between Venus and the Earth is a minimum. The flux density of Venus was close to its maximum value early in April, but it was decreasing each day as the planet's orbital motion carried it farther from Earth. In fact, the intensity of Venus varies by a factor of *thirty eight* as the planet's distance varies from 0.28 to 1.72 astronomical units.

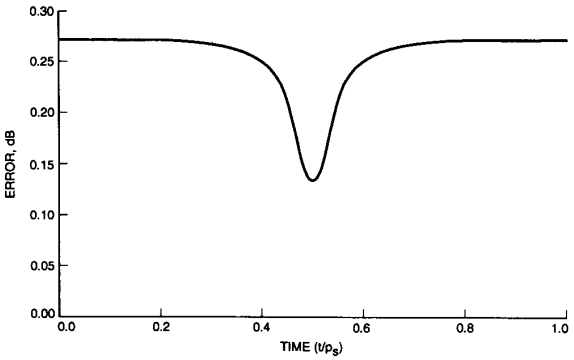

Fig. 7. Relationship between calculated error in $G/T_{\rm op}$ and the orbital period of Venus for measurements of the planet using a radiometer receiving system with a hypothetical 11% nonlinearity.

Figure 7 shows the predicted error that would result if measurements of Venus were used to calibrate $G/T_{\rm op}$ for the 34-m BWG antenna at 33.68 GHz using a TPR receiving system that is 11% nonlinear. The plot shows the absolute error that would be expected as a function of the planet's 19-month synodic period P_s and the time of the observations t (months). Note that the error is a minimum (0.14 dB) near $x = t/P_s = 0.5$, when Venus is closest to Earth and that it increases to 0.27 dB as Venus reaches maximum distance at $x = 1$ (Superior Conjunction). If measurements were spread over this time span, $G/T_{\rm op}$ would appear to vary as much as 0.13 dB.

As an example of the effect of nonlinear receiving system errors, consider a hypothetical experiment whereby a nonlinear TPR is used to measure the brightness temperature of Venus. If the experimenter were unaware of the nonlinearity, the variations in systematic error shown in Fig. 7 might be mistakenly attributed to changes in the brightness temperature of the planet. In fact, the variation might readily be accepted as evidence of a phase angle dependence because the error-induced variability is so tightly coupled with the orbital period.

V. Conclusion

The sensitivity of DSN receiving systems has dramatically increased as a result of three decades of technological advances and improved engineering practices. To realize the benefits of high sensitivity, it is important that receiving systems are accurately calibrated and that $G/T_{\rm op}$ measurements are repeated over time to maintain peak performance. The method described in this paper is designed to measure system performance in terms of $G/T_{\rm op}$ and includes a technique to calibrate the radiometer system using procedures, software, and commercial instruments that are easy to implement and efficient to use. The radiometer calibration only requires a few minutes to complete and the $G/T_{\rm op}$ measurements are typically accomplished in about 10 h.

The utility of the calibration technique and the measurement procedure was demonstrated by performing tests on receiving systems operating at K_a-band frequencies on the 34-m BWG antenna at DSS 13. One of the tests consisted of observing calibration radio sources over a wide range of elevation angles. The observations were made by interleaving system radiometer calibrations with radio source intensity measurements, which were accomplished using an automatic boresight technique. Three calibration radio sources were selected to validate the use of multiple sources to measure the dependence of $G/T_{\rm op}$ on radio source elevation angle. The advantage of multiple radio sources is the ability to measure $G/T_{\rm op}$ at many azimuth and elevation angles in a single observing session of 8–12 h.

A plot of the observational data produced a smooth curve of antenna aperture efficiency versus elevation angle that peaked at 43% near 55° elevation angle. The corresponding peak antenna gain is $G = 77.94$ dB at 33.86 GHz. The results from the three different radio sources are mutually consistent even though their relative intensities ranged from 1.5 to 105 K.

An important component of the TPR system calibration method concerns the receiving system linearity, which is measured and quantified with sufficient accuracy that the impact on system performance can be assessed. The analysis of the experimental data showed that $G/T_{\rm op}$ can be measured with a 2-sigma precision of the order $\pm$ 0.15 dB if the receiving system is linear. The analysis also indicated that even modest ($< 10\%$) TPR nonlinearity can affect the absolute measurement accuracy as much as $\pm$ 0.5 dB and can lead to discrepancies in the measurement of system temperature ($T_{\rm op}$) and $G/T_{\rm op}$.

Receiving system nonlinearities are frequently overlooked as an error source in the calibration of microwave radiometers and antenna measurements. The experimental results described in this paper illustrate some of the ways that radiometer nonlinearity can negatively impact system performance calibration. The calibration techniques and analysis provide quantitative information that enables the system engineer to adjust and linearize the receiver. When that is not practical, the experimenter or the operator can apply correction coefficients to the measured values of $T_{\rm op}$ and thereby compensate for the radiometer nonlinearity.

Although this paper concentrated on a TPR, the radiometer calibration method is generic. The details will depend upon the specific parameters of the receiving systems including the choice of calibration loads. For example, the effect of receiving system nonlinearity for a radiometer using a room-temperature calibration aperture load will differ from a system using a liquid-nitrogen-cooled calibration load. The value of the technique is the ease with which it can be implemented and used to measure and monitor system performance.

Appendix
Radiometer Equations and Application to Receiving System Nonlinearity Correction and Error Analysis

A. Radiometer Equations

The equations for calibrating radiometer receiving system gain and accounting for nonlinearity are developed in the

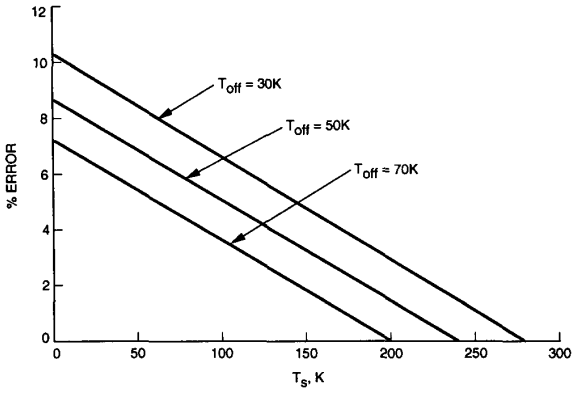

Fig. 8. DSS-13 34-m antenna radio source difference calibration measurement errors using an unoptimized radiometer receiving system with about 11% nonlinearity and assuming various off source system noise temperatures.

following. The results are applicable to not only the TPR but to NAR, Dicke, and other radiometer configurations.

Consider the TPR shown in Fig. 8. The calibration method consists of recording the receiving system output readings designated $R1, R2, R3, R4$, and $R5$: output device input terminated, receiver input switched to the antenna, antenna + calibration noise diode (ND), ambient load, and ambient load + ND, respectively. The readout device offset $R1$ is subtracted from the original $R2, R3, R4$, and $R5$ readings. The offset corrected readings $R2, R3, R4$, and $R5$ correspond to system noise temperatures $T2, T3, T4$, and $T5$ in the following analyses. A linear analysis assumes equations of the form

$$T = BR \tag{A1}$$

where

- T system noise temperature with radiometer receiver
- $T4$ $= 273.16 + T_p + T_e - T_cf$ (K)
- T_p ambient load temperature (°C)
- T_cf $= 0.024$ F (GHz) (high-frequency noise temperature correction)
- T_e receiving system noise temperature $= T_{\text{lna}} + T_f$ (K)
- T_{lna} LNA noise temperature (K)
- T_f follow-on amplifier noise temperature contribution
- R radiometer receiver output device readings with receiving system input connected to the designated source defined for T (W) (typ)
- B receiving system gain $= T4/R4$ (K/W) (typ)

The system noise temperature $T2(= T_{\text{op}})$ with the receiving system LNA input connected to the antenna is defined previously with (8).

T_f is measured periodically [26] and T_{lna} is assumed calibrated in the laboratory or field environment [4]. From readings $R3$ and $R5$, measurements of the system noise temperatures $T3$ and $T5$ are obtained. The noise temperature of the ND is measured with the receiver input connected to the antenna and to the ambient load as $TN2 = T3 - T2$ and $TN4 = T5 - T4$. The analysis to quantify and correct the receiving system nonlinearity assumes a quadratic nonlinear corrected solution for system noise temperature TC in terms of the linear solution T.

$$TC = BC \cdot T2 + CC \cdot T2^2 \tag{A2}$$

using the measured noise temperatures from the linear analysis

$$T2C = BC \cdot T2 + CC \cdot T2^2 \tag{A3}$$

$$T3C = BC \cdot T3 + CC \cdot T3^2 \tag{A4}$$

$$T4 = BC \cdot T4 + CC \cdot T4^2 \tag{A5}$$

$$T5C = BC \cdot T5 + CC \cdot T5^2. \tag{A6}$$

$TC4$ has been replaced with $T4$ since this is a condition for setting the radiometer receiving system gain. Forcing equality for the corrected noise diode temperature TNC on the antenna and ambient load

$$TNC = T3C - T2C \tag{A7}$$

$$TNC = T5C - T4. \tag{A8}$$

The constants BC and CC are given by (A9) and (A10) below. For a highly linear radiometer receiving system, CC approaches 0 and BC approaches 1. A radiometer receiving system linearity factor is defined by

$$FL = T2C/TC. \tag{A11}$$

B. Radiometer Programs and Application

These equations have been programmed in computer spreadsheet applications as RADPRE for radiometer precalibrations and RADOBS for observing calibrations. The input data format is the same for each program. The data can be formatted in CSV (comma separated value) files. Typically, six sets of data are recorded for RADPRE in less than 10 min. The observing calibrations, analyzed with program RADOBS usually involve calibrations over many hours, appropriate for the users observing activities. Calibrating and monitoring the radiometer receiving system gain and linearity changes are important for the observing measurements accuracy and consistency. Typically, the system hardware is maintained for suitable linearity and only the radiometer receiving system gain changes are used for correcting the observational data.

$$CC = \frac{T5 - T4 - T3 + T2}{T4(T5 - T4 - T3 + T2) - (T5^2 - T4^2 - T3^2 + T2^2)} \tag{A9}$$

$$BC = 1 - CC \cdot T4. \tag{A10}$$

C. The Error in Radio Source Difference Measurements

These following equations can be used to estimate the error due to receiving system nonlinearity in radio source antenna pointing "on–off" measurements. Assuming the linear analysis is in error and the nonlinear is not (an approximation), the percentage error for a radio source difference measurement is given by

$$\% \text{ error} = 100((T_s/T_sC) - 1) \tag{A12}$$

where

T_s $= (T_{\text{on}} - T_{\text{off}})$, K
T_sC $= (T_{\text{on}}C - T_{\text{off}}C)$, K
T_{on} system noise temperature, on source, K
T_{off} system noise temperature, off source (same sky region), K
$T_{\text{on}}C$ system noise temperature, corrected, on source, K
$T_{\text{off}}C$ system noise temperature, corrected, off source, K

using (A3) and

$$T_{\text{on}}C = BC \cdot T_{\text{on}} + CC \cdot T_{\text{on}}^2 \tag{A13}$$

$$T_{\text{off}}C = BC \cdot T_{\text{off}} + CC \cdot T_{\text{off}}^2 \tag{A14}$$

with (A10) and (A12) and $T_{\text{on}} = T_s + T_{\text{off}}$

$$\% \text{ error} = \frac{100\,CC(T4 - T_s - 2T_{\text{off}})}{1 - CC\,(T4 - T_s - 2T_{\text{off}})}. \tag{A15}$$

Equation (A15) is a maximum at $T_s = 0$ and goes to zero if $CC = 0$ or

$$T_s = T4 - 2T_{\text{off}}. \tag{A16}$$

The % error (A15) is shown in Fig. 8 using the radiometer constants for the DSS 13 34-m antenna K_a-band TPR prior to optimizing the radiometer receiving system linearity (measured 11/10/92, $CC = 3.33394 \times 10^{-4}$ and $T4 = 340.08$ K) for $T_{\text{off}} = 30$, 50, and 70 K. These T_{off} temperatures approximate the K_a-band zenith system noise temperatures for future maser, present maser, and present HEMT LNA operation, respectively. This plot shows that the nonlinearity is maximum for low system and source noise temperatures and minimum for (A16) satisfied. The radio source measurement errors are discussed further in the text.

ACKNOWLEDGMENT

L. Skjerve provided most of the Goldstone Venus station TPR software installation. The Venus station operational support was provided by C. Goodson, A. Price, G. Bury *et al.* The tropospheric attenuation software was provided by S. Slobin.

REFERENCES

[1] W. Rafferty *et al.*, "Ground antennas in NASA's deep space telecommunications," this issue, pp. 636–645.
[2] D. F. Wait *et al.*, "A study of the measurement of G/T using Cassiopeia A," NBS AD-785 433, June 1974.
[3] "IRE Standards on Electron Tubes: Definitions of Terms, 1962 (62 IRE 7.S2)," *Proc IEEE*, vol. 61, pp. 434–442, Mar. 1963.
[4] C. T. Stelzried, "The deep space network: Noise temperature concepts, measurements, and performance," JPL Pub. 82-33, Jet Propulsion Lab., Pasadena CA, Sept. 15, 1982.
[5] S. Silver, *Microwave Antenna Theory and Design.* New York: McGraw-Hill, 1949.
[6] K. Bartos *et al.*, "Antenna gain calibration procedure," JPL Internal Doc. D-3794, Nov. 15, 1986.
[7] W. M. Baars *et al.*, "The absolute spectrum of Cas A; An accurate flux density scale and a set of secondary calibrators," *Astron. Astrophys.* , p. 106, 1977.
[8] J. A. Turegano and M. J. Klein, "Calibration radio sources for radio astronomy: Precision flux density measurements at 8420 MHz," *Astron. Astrophys.*, p. 86, 1980.
[9] M. J. Klein and C. T. Stelzried, "Calibration radio sources for radio astronomy: Precision flux-density measurements at 2295 MHz," *Astron. J.*, Dec. 1976.
[10] M. J. Klein and A. Freiley, "DSN radio source list for antenna calibration," JPL Internal Doc. D-3801 Rev. B, Sept. 25, 1987.
[11] P. D. Batelaan, R. M. Goldstein, and C. T. Stelzried, "A noise adding radiometer for use in the DSN," JPL Space Programs Summary 37-65, vol. II, pp. 66–69, Sept. 30, 1970.
[12] C. T. Stelzried *et al.*, "DSS-13 26-m antenna upgraded radiometer system," JPL TDA PR 42–109, May 1992.
[13] C.T. Stelzried, "Microwave radiometer calibrations," JPL Doc. D-10496, Jan. 29, 1993.
[14] L. J. Skjerve, "Preliminary documentation for DSS 13 radiometer program," JPL Internal Doc. D-9292, Jan. 1990.
[15] C. T. Stelzried, "Operating noise-temperature calibrations of low-noise receiving systems," *Microwave J.*, vol. 14, no. 6, p. 41, June 1971.
[16] ——, "Noise adding radiometer performance analysis," TDA PR 42-59, pp. 98–106, Oct. 1980.
[17] ——, "Non-linearity in measurement systems: evaluation method and application to microwave radiometers," JPL TDA PR 42–91, Nov. 1987.
[18] P. G. Steffes, M. J. Klein, and J. M. Jenkins, "Observations of the microwave emission of Venus from 1.3 to 3.6 cm," *Icarus*, no. 84, pp. 83-92, 1992.
[19] M. J. Klein and S. Gulkis, "Jupiter's atmosphere: Observations and interpretation of the microwave spectrum near 1.25-cm wavelength," *Icarus* , no. 35, pp. 44–60, 1978.
[20] I. dePater and S. T. Massie, "Models of the millimeter–centimeter spectra of the giant planets," *Icarus*, no. 62, pp. 143–171, 1985
[21] F. T. Ulaby *et al.*, *Microwave Remote Sensing Active and Passive*, vol. 1. Reaading, MA: Addison-Wesley, 1981
[22] M. Britcliffe *et al.*, "DSS-13 Beam Waveguide Antenna Project," Phase I Final Rep., JPL Internal Doc. D-8451, May 15, 1991.
[23] M. S. Gatti, M. J. Klein, and T. B. H. Kuiper, "32 GHz performance of the DSS-14 70-meter antenna: 1989 Configuration," JPL TDA PR 42-99, Nov. 1989.
[24] J. S. Shell *et al*, "Ruby masers for maximum G/T_{op}," this issue, pp. 796–810.
[25] C. T. Stelzried, "Correction of high frequency noise temperature inaccuracies," JPL TDA PR 42–111, Nov. 15, 1992.
[26] ——, "Improved RF calibration techniques: daily system noise temperature measurements," JPL Space Programs Summary 37–42, vol III, Nov. 30, 1966.

Charles T. Stelzried (Senior Member, IEEE) received the Ph.D. degree in engineering from the University of Southern California, Los Angeles, in 1969.

He has been at the Jet Propulsion laboratory, Pasadena, CA, continuously since 1953. From 1967 to 1981 he was involved with deep-space radio science as a team member of the NASA Marriner 10, Viking, and Helios missions. From 1981 to 1986 he was the Tracking and Data Systems (TDA) Manager for the Ulysses, Mag-

ellan, Giotto, Venus Balloon, and Vega Pathfinder deep-space missions. Since 1986 he has been the Deputy Program Manager of Advanced Systems for the NASA/JPL Deep Space Network (DSN). This program has responsibility for research areas applicable to deep-space missions including microwave and optical communications systems, radiometric technology for navigation, and orbital debris radar. His fields of special interests include low-noise amplifier, noise calibration techniques, and use of the DSN as a science instrument. He has been involved with the DSN low-noise receiving systems since the first JPL Venus Radar Experiment in 1961. He has 57 publications, numerous JPL/NASA internal reports, Tech Briefs, and 5 patent disclosures, including the Multi-feed Cone Cassegranian Antenna configuration presently used in the Deep Space Network and numerous NASA awards, including the Exceptional Scientific Achievement medal.

Dr. Stelzried is a member of Tau Beta Pi, AAAS, Sigma Xi, and URSI Commission A.

Michael J. Klein was born in Ames, IA, in 1940. He received the B.S.E.E. degree from Iowa State University, Ames, in 1962, and the M.S. and Ph.D. degrees in radio astronomy from the University of Michigan, Ann Arbor, in 1966 and 1968, respectively.

In 1968 he was awarded a Resident Research Associateship at the Jet Propulsion Laboratory (JPL), Pasadena, CA, by the National Research Council. He joined JPL in 1969 as a Scientist in the Space Science Division and became supervisor of the Radio Astronomy Group in 1974. From 1981 to 1993 he was the JPL Program Manager for NASA's Search for Extraterrestrial Intelligence (SETI), a project conducted by the NASA–Ames Research Center and JPL. He is currently Manager of the JPL Office for Astronomical Studies of Extrrasolar Planetary Systems (ASEPS), which is a NASA research program in its formative stages to detect and characterize planets orbiting other stars. He is a recipient of a NASA Exceptional Achievement Medal. In 1993, he was awarded a Professional Achievement Citation in Engineering from Iowa State University College of Engineering.

Dr. Klein is a member of Eta Kappa Nu, Sigma Xi, the International Astronomical Union (IAU), the American Astronomical Society (AAS), the International Scientific Radio Union (URSI), and the American Institute of Aeronautics and Astronautics (AIAA). He is a past chairman of the AIAA Technical Committee on Space Science and Astronomy.